Available online at www.sciencedirect.com
ScienceDirect
Ceramics International 37 (2011) 1093–1099
CERAMICS INTERNATIONAL
www.elsevier.com/locate/ceramint

Thermal properties of plasma-sprayed thermal barrier coating with bimodal structure

Qinghe Yu [a,b], Abdul Rauf [a,b], Na Wang [a,b], Chungen Zhou [a,b,*]

[a] School of Materials Science and Engineering, Beijing University of Aeronautics and Astronautics, Beijing 100191, China
[b] Key Laboratory of Aerospace Materials and Performance (Ministry of Education), China

Received 23 June 2010; received in revised form 19 September 2010; accepted 20 November 2010
Available online 25 December 2010

Abstract

Nanostructured zirconia coatings have been prepared by atmospherical plasma spraying (APS) on NiCrAlY-coated superalloy substrates. The isothermal oxidation test results indicate that the oxidation kinetics of nanostructured TBC follows a parabolic law and the oxidation resistance of the nanostructured TBC is comparable to that of the conventional TBC. The nanostructured thermal barrier coatings exhibit excellent thermal cyclic resistance and low thermal diffusivity. The failure of the nanostructured TBC occurs within the top coat and close to the YSZ/thermal growth oxide interface. The thermal diffusivity of the coating is 90% of that of conventional thermal barrier coatings, and it increases after heat treatment at 1050 °C for 34 h. The increase in the thermal diffusivity of the coating is ascribed to grain growth, the crack healing as well as sintering neck formation.

Keywords: Nanostructure; Thermal barrier coating; Thermal diffusivity; Oxidation

1. Introduction

Plasma-sprayed thermal barrier coatings are traditionally applied to turbine engine blades and vanes in order to reduce their operating temperatures and increase the component durability. A typical duplex TBC system consists of a thermally insulating ZrO_2 alloy top coat applied over an oxidation-resistant MCrAlY (M = Ni and/or Co) bond coat. However, conventional TBC usually suffers premature failure during thermal and mechanical loading, and this is attributed to their poor bond strength and high residual stresses. In order to release the residual stresses and improve the service life and insulation effect of TBC, the nanostructured thermal barrier coating was proposed [1–9].

The thermal properties of TBCs need to be investigated extensively as these coatings are used at extremely high temperature and severe thermal loads. The service life of plasma-sprayed TBC is closely related to such factors as thermal cycling resistance, oxidation resistance of bond coat, and the thermal expansion mismatch strains [10]. Plasma-sprayed nanostructured thermal barrier coatings are built up by successive accumulation of partially molten powder particles. Therefore, the thermal properties of plasma-sprayed nanostructured TBC are different from those of conventional TBC. There are many reports on the thermal properties of traditional thermal barrier coatings [11–14]. However, few reports on plasma-sprayed nanostructured zirconia coatings have been published. A study concerning the thermal cyclic life and thermal diffusivity of nanostructured TBC was conducted by Zhou et al. [15]. The thermal cyclic life and thermal diffusivity of the coating are more than 1.5 times and 90% of those of conventional APS TBCs, respectively. The excellent thermal cycling resistance for the coating can be attributed to the increase in cohesive strength, and the micro-pores between the powders, which can adsorb the residual stress. The lower thermal diffusivity is explained in terms of the decreased grain size of nanostructured zirconia coatings. However, the oxidation behavior of the coating and influence of heat treatment on the thermal diffusivity of the coating, have not been reported so far. With the above background, the present study deals with the oxidation behavior and influence of heat

* Corresponding author at: School of Materials Science and Engineering, Beijing University of Aeronautics and Astronautics, Beijing 100191, China. Tel.: +86 108 2338622; fax: +86 10 82338200.
E-mail address: cgzhou@buaa.edu.cn (C. Zhou).

0272-8842/$36.00
doi:10.1016/j.ceramint.2010.11.033

treatment on the thermal diffusivity of the coating for providing the relevant knowledge.

2. Experimental procedures

2.1. Preparation of TBCs

The substrates were cut into coupons with a dimension of 15 mm in diameter and 2 mm in thickness from a wrought sheet of nickel-based superalloy with nominal composition (wt.%) of Ni–10Co–9.0Cr–2.0Mo–7.0W–5.2Al–0.9Ti–3.8Ta–1.5Hf (DZ125). These coupons were grit-blasted, using 250-μm alumina grit, to obtain a sharp-peaked surface contour with a roughness average of 4–5 μm, in order to improve the adherence of the coating. The powder materials used for spraying were Ni–22Cr–10Al–lY used for the bond coats and ZrO_2–$8Y_2O_3$ for the ceramic coats. The $8\%Y_2O_3$ partially stabilized nanostructured zirconia powder, having grain size of 30–50 nm, was used as the starting powder as shown in Fig. 1(a)

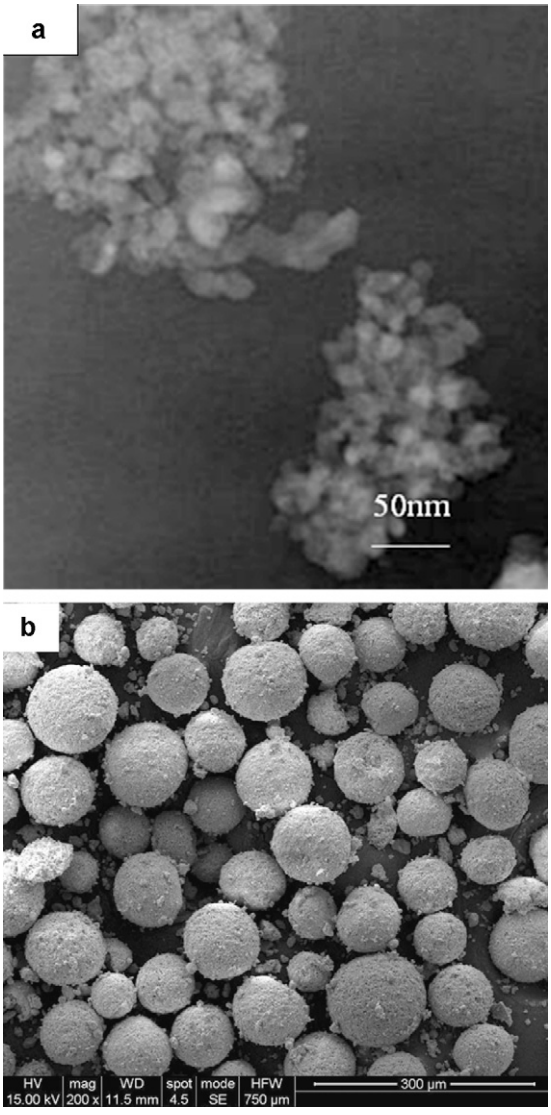

Fig. 1. The TEM image of starting nano-YSZ powder (a) and the SEM image of spray dried nano-YSZ powder (b).

Table 1
Plasma-sprayed parameters for bond coating and nanostructured zirconia coating.

	NiCrAlY bond coating	Zirconia coating
Primary gas Ar (slpm)	60	60
Secondary gas H_2 (slpm)	20	15
Carrier gas Ar (slpm)	3.5	4.5
Gun current (amp)	580	600
Gun voltage (V)	60	63
Spray distance (mm)	290	80
Powder feed rate (g/min)	45	25

and was reconstituted into spherical micrometer-sized granules (typical size range in 40–60 μm) (Fig. 1(b)) by spray-drying process before plasma spraying in this experiment. The bond coating was sprayed with low pressure plasma spraying (LPPS) and air plasma spraying (APS) was used to prepare the nanostructured zirconia coating. The nanostructured powder particles are required to be molten partially to keep bimodal structure after the solidification of surface coatings. The parameters used to get the bimodal structure have been investigated in the previous investigation [16]. The parameters for plasma spraying in the present study were shown in Table 1. The ranges of thickness of bond coats and ceramic coats were 80–100 μm and 200–250 μm, respectively. For comparison, the conventional thermal barrier coating with the same thicknesses of bond coat and ceramic layer as that of nanostructured TBC were produced under the same plasma spraying parameters as that of the nanostructured thermal barrier coating, and the bond coat for the conventional coating were produced in the same batch with nanostructured coating.

2.2. Isothermal oxidation

The sample was coated on all sides and the isothermal oxidation tests were carried out at 1050 °C in static air. The specimens were placed in alumina crucibles, oxidized at 1050 °C and then cooled to room temperature at regular intervals for mass measurements. The sensitivity of the balance used was 0.1 mg. Three measurements of weight gain at each time were taken and averaged. The oxidation behavior was evaluated by the weight gain of the samples.

2.3. Cyclic oxidation

Cyclic oxidation tests were conducted for the evaluation of thermal cycling life of the coatings. The cyclic oxidation tests were performed under atmospheric pressure at 1050 °C in static air. Each cycle consisted of an hour immersion in the furnace followed by a 10 min cooling down to room temperature. A sample was considered to have failed when spallation was seen visually.

2.4. Thermal diffusivity measurement

The samples were machined to disk shape (10 mm in diameter and 1 mm in thickness) along the direction parallel to

the coating surface for thermal diffusivity measurements. The measurements of the variation of the thermal diffusivity, from room temperature up to 800 °C, were carried out according to the ASTM C-1113 standard through laser equipment (TC-3000H) from SINKU-RICO. The laser-flash diffusivity method was used before and after annealing at 1050 °C for 34 h in the temperature range from room temperature to 800 °C. In order to assure complete absorption of the laser-flash at the sample surface and measurement of the transient temperature at the opposite surface, the coating samples were coated both sides with a carbon film before the measurement. For comparison, the traditional zirconia coatings sprayed at the same parameters as nanostructured zirconia coating were also measured. Three measurements of thermal diffusivity were taken for each sample at each temperature and averaged.

2.5. Microstructure analysis

The microstructures of the nanostructured zirconia coatings before and after oxidation were observed with an S-3500 scanning electron microscope (SEM, Hitachi, Tokyo, Japan). The porosity of YSZ coating was tested by mercury porosimetry method, using AUTOPORE II 9220 V3.04, which was made by Micromeritics Inc., USA.

3. Experimental results and discussion

3.1. Microstructure of as-sprayed nanostructured YSZ coating

Fig. 2 is the fractured cross-section morphology of as-sprayed nanostructured YSZ coating. As shown in Fig. 2, the observed cross-sectional microstructure is typical of APS nanostructured coatings with dense area (melted area), microcracks, high volume spheroidal pores, splats and nanozones (unmelted or partially melted particles). According to the cross-section of the nanostructured YSZ coatings, the percentage of non-molten particles exhibited in the coatings is about 35 ± 8% determined by the scanning electron microcopy and image analysis. The porosity of the nano-YSZ coating is about 24% tested by mercury porosimetry method. The porosity is composed of micropores (diameter < 1 μm) and macropores (diameter > 1 μm). As shown in our group's work [17], the ratio of the micropores and the macropores is about 20% and 4%, respectively. Micropores contribute a larger percentage of the total porosity than macropores. The grain size of the nanostructured coating is ranging from 70 to 100 nm [15] and the thickness of the coating is about 200 μm.

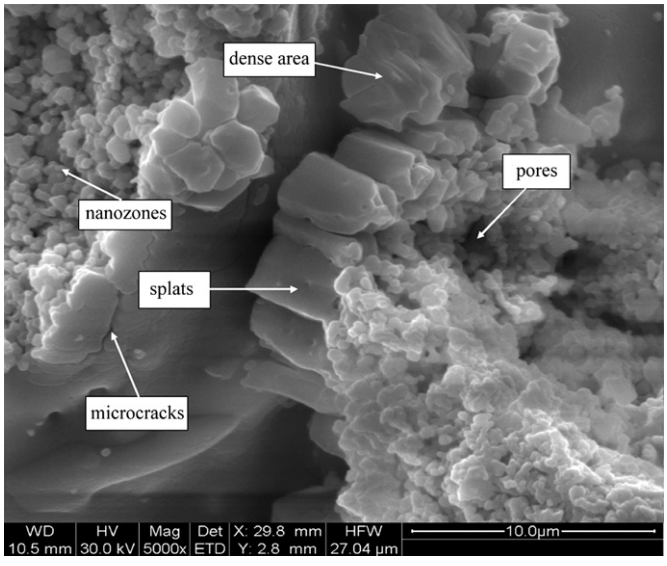

Fig. 2. The fractured cross-section morphology of as-sprayed nanostructured YSZ coating.

3.2. Isothermal oxidation kinetics

Fig. 3(a) shows the weight gain as a function of time for nanostructured TBCs at 1050 °C in static air. In the early stage of the oxidation, the selective oxidation occurred, so the weight gain is higher. The weight gain is 1.47 mg/cm^2 after isothermal oxidation for 40 h. After about 50 h, the weight gain becomes flat. Finally the weight change per unit area was about 1.85 mg/

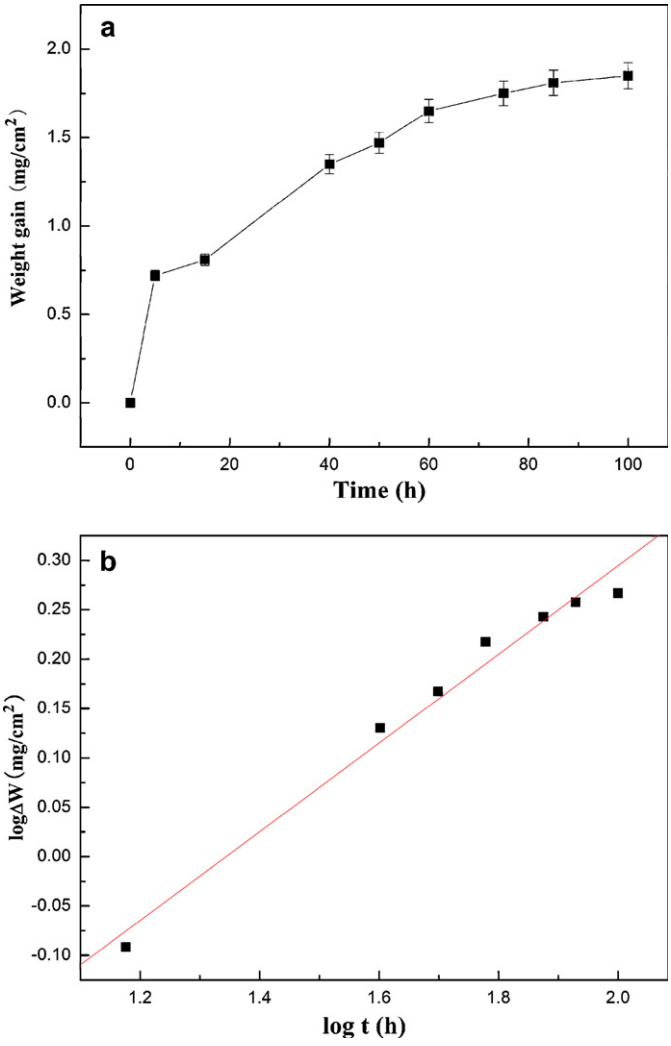

Fig. 3. (a) Isothermal oxidation kinetics of nanostructured TBC at 1050 °C in static air, (b) variation of logarithm of weight gain with logarithm of time.

cm^2 after isothermal oxidation for 100 h at 1050 °C. The oxidation kinetics can be quantified further in terms of oxidation exponent, n and rate constant k_p obtained from the relation:

$$\Delta W^n = k_p t$$

where ΔW is the weight change per unit area of the specimen and t is the exposure time. Fig. 3(b) shows the variation of $\log \Delta W$ against $\log t$ for the nanostructured YSZ sample at 1050 °C. The slope of the nanostructured YSZ coating sample is calculated as 0.46 ($n \approx 2$) in the $\log \Delta W - \log t$ plot. This means that the oxidation process of the nanostructured coating obeys the parabolic rate law. The parabolic rate constant ($mg^2\,cm^{-4}\,h^{-1}$) at 1050 °C is calculated to be $k_p = 0.05$. For comparison, the weight gain of conventional plasma sprayed TBC, which only differs in the ceramic top coat microstructure, was measured. The weight gain of the conventional TBC after isothermal oxidation for 100 h at 1050 °C was about 1.75 mg/cm^2. Compared with traditional YSZ coatings, there are much more micropores existed in the nano-YSZ coatings, the nanostructured YSZ coatings are looser and had a higher porosity (24%) than that of traditional YSZ coatings (10%). This looser structure in the nano-YSZ coating makes it easier for the transport of oxygen ions. As a consequence, the weight gain per unit area of the nanostructured TBC after isothermal oxidation for 100 h at 1050 °C is a little higher than that of conventional TBC coating.

3.3. Thermal cycling lifetime

Fig. 4 compares the thermal cycling lifetime of plasma sprayed nanostructured thermal barrier coating and conventional plasma sprayed TBC, which only differs in the ceramic top coat microstructure. The lifetimes of nanostructured and conventional thermal barrier coatings are about 600 cycles and 400 cycles, respectively. The result indicates that the thermal cycling life of the plasma sprayed nanostructured thermal barrier coating is more than 1.5 times of those of conventional APS TBCs. The improvement in the thermal cycling resistance of the nanostructured thermal barrier coating can be attributed

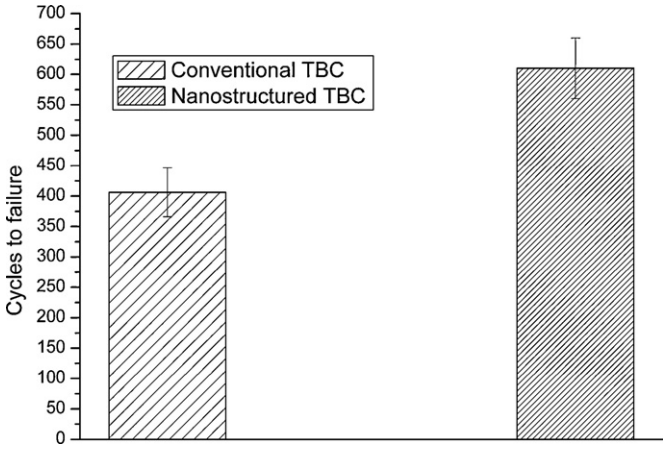

Fig. 4. Thermal cyclic life of nanostructured TBC and conventional TBC.

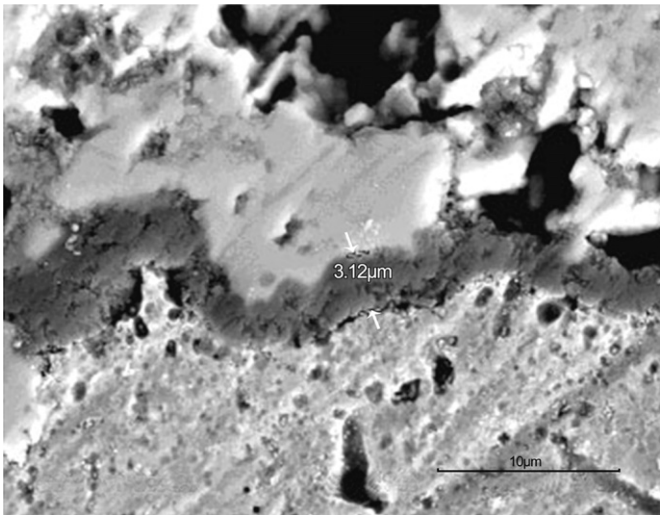

Fig. 5. Cross-section of nanostructured thermal barrier coating after isothermal oxidation at 1050 °C for 100 h.

to the absorption of the residual stress and the increase in cohesive strength [15].

3.4. Morphologies after isothermal oxidation at 1050 °C in air for 100 h

Fig. 5 shows cross-sectional images of the oxides formed along the bond coat and top coat interface after isothermal oxidation at 1050 °C in air for 100 h. It is seen that the morphologies of the oxides formed after oxidation were continuous and dense. Fig. 6 shows the micrograph and corresponding X-ray maps of Al, O, Cr, Ni and Zr of polished cross-section of the oxide scales along the bond coat and top-coat interface after isothermal oxidation at 1050 °C in static air for100 h. Element-distribution map analysis on the oxide formed in air revealed strong profile of Al and O, indicating that the oxide was mainly composed of Al_2O_3. A layer of Al_2O_3 between the top coat and the bond coat may prevent the coating from further oxidation. Fig. 7 shows the cross-sectional micrograph of the nanostructured thermal barrier coating after cyclic oxidition at 1050 °C for 610 cycles. It is seen from Fig. 7 that there are some lateral cracks which were initiated near the interface of YSZ top layer and thermal growth oxide. The failure of the nanostructured TBC occurs within the top coat and close to the YSZ/thermal growth oxide interface. Chang et al. [18] reported that the spalling occurred through the ceramic layer and bond coat internal oxide interface. The result indicates that the failure of the nanostructured TBC is similar to the failure scenario of conventional APS TBCs.

3.5. Thermal diffusivity

Fig. 8 presents the thermal diffusivity of conventional zirconia coating and the as-sprayed nanostructured zirconia coatings before and after heat treatment at 1050 °C for 34 h during the temperature from room temperature to 800 °C. It can be seen that the thermal diffusivity of both coatings decreases slightly with increasing temperatures. The thermal

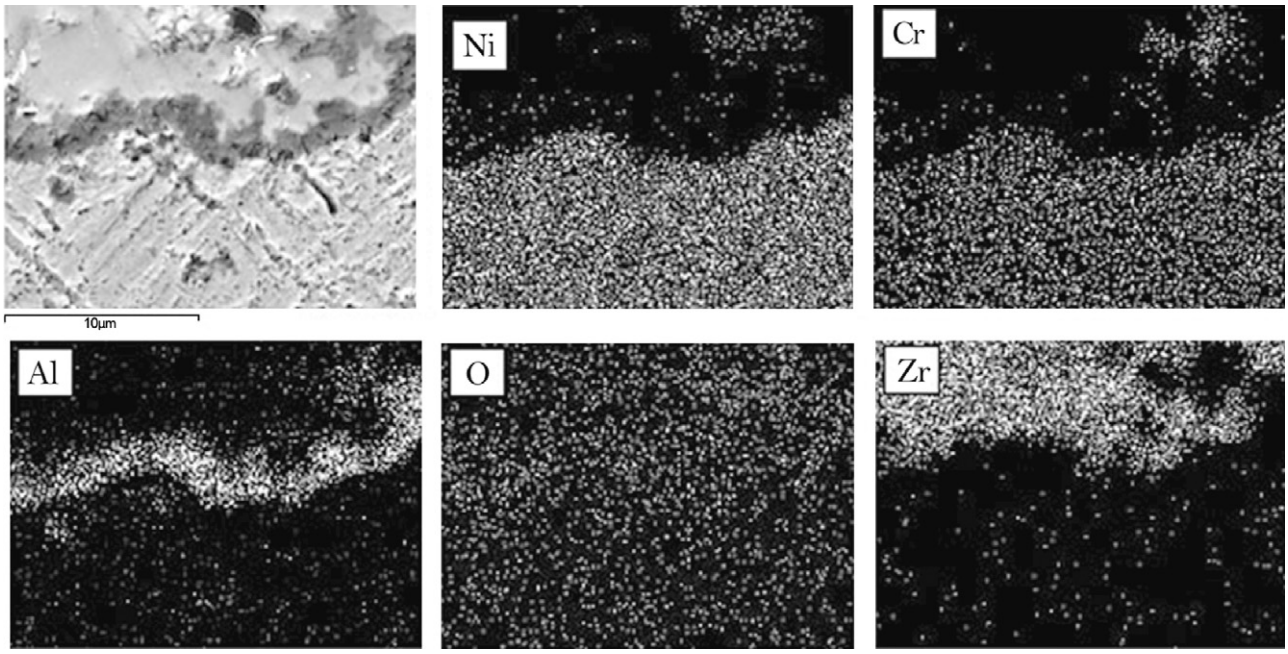

Fig. 6. Microstructure and X-ray mappings of Al, O, Cr, Ni and Zr of polished cross-section of the oxides at NiCrAlY/YSZ interface after oxidation at 1050 °C in static air for 100 h.

diffusivity of nanostructured zirconia coating in the as-sprayed is in the range of 2.15–2.75 × 10^{-7} m^2/s during the temperature from room temperature to 800 °C, thermal diffusivity of the conventional zirconia coating is 2.35–2.96 × 10^{-7} m^2/s, while thermal diffusivity of nanostructured zirconia coating after heat treatment at 1050 °C for 34 h was 2.50–3.15 × 10^{-7} m^2/s. The thermal diffusivity of the plasma-sprayed nanostructrued zirconia coating is lower than that of the conventional zirconia coating. The thermal diffusivity of the plasma-sprayed nanostructrued zirconia coating increases after heat-treatment at 1050 °C for 34 h. It is known from the above results that the thermal diffusivity of the plasma-sprayed nanostructrued zirconia coating is lower than that of conventional TBC, and increases after heat-treatment at 1050 °C for 34 h. Compared with conventional TBC, the decrease in the thermal diffusivity of the nanostructured TBC is attributed to the decreased grain size of nanostructured zirconia coatings. At temperature below 1200 °C, phonon transport dominates the heat conduction through zirconia. For conventional materials, the grain boundary contribution to phonon scattering is thought to be small [19,20]. However, when the grain size is of the same order as the mean free path for phonon scattering, grain boundaries can have a significant effect.

The grain-boundary scattering in nanostructured coatings can be expressed as follows:

$$l_b = \frac{20T_m\alpha}{T\gamma^2} \quad (1)$$

where l_b is the phonon mean free path, T_m is the absolute melting temperature, α is the lattice constant, and γ is the

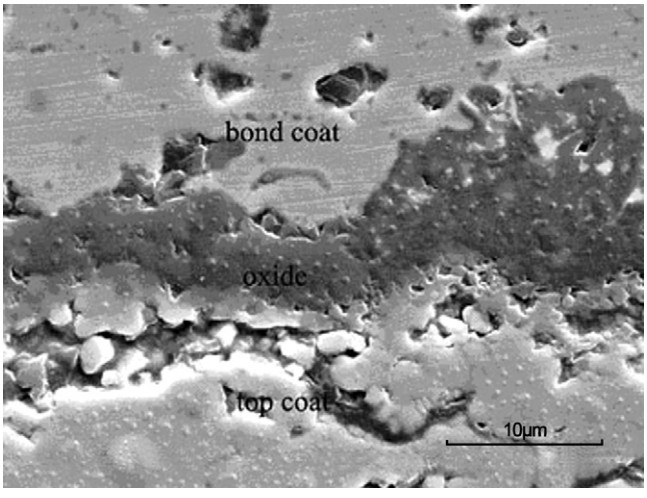

Fig. 7. Cross-section of nanostructured thermal barrier coating after cyclic oxidation at 1050 °C for 610 cycles.

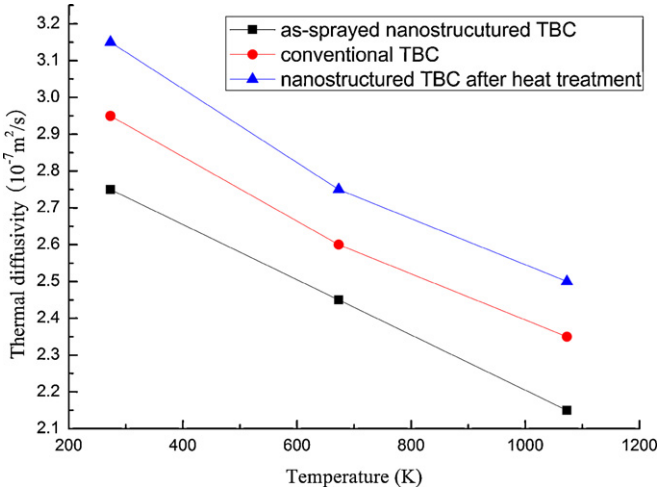

Fig. 8. Thermal diffusivity of conventional zirconia coating and the as-sprayed nanostructured zirconia coating before and after heat treatment at 1050 °C for 34 h.

Gruneisen constant. Using this relation, l_b for single crystal YSZ is calculated to equal 25 nm at 300 K [21]. The grain size of as-sprayed coatings in the present study is about 50 nm [2], and the reduction in thermal diffusivity of the nanostructured YSZ coating due to phonon scattering by grain boundaries will become significant for grain size comparative to l_b. Meanwhile, higher porosity of the nanostructured YSZ coating also contributes to the lower thermal diffusivity. The porosity of the nanostructured and traditional YSZ coating is about 24% and 10%, respectively. The micropores in the nanostructured coating are smaller in size. The smaller the micropores are, the more interfaces are produced, and the effect on the phonon scattering is higher, resulting in the reduction of thermal diffusivity [22]. As a synergistic effect of grain boundary and micropores, the thermal diffusivity of the nanostructured YSZ coating decreased.

The grain size of the nanostructured YSZ coating after heat treatment at 1050 °C for 34 h is increased from about 50 nm to 100 nm by our previous investigations [2–23]. Phonon scattering by grain boundaries will become less significant due to the grain growth. In addition to the increase in grain size, the increase in the thermal diffusivity after the heat treatment at 1050 °C for 34 h is attributed to the decrease in the porosity of the coating. The porosity of as sprayed nanostructured coating before and after heat treatment at 1050 °C for 34 h is 24% and 20%, respectively. Cernuschi et al. [24] investigated the effect of sintering on the thermal diffusivity of thermal barrier coating. The results showed a significant increase of the thermal diffusivity after exposure of few hours, especially at the high testing temperatures. Microstructural analysis carried out by optical and electron microscopy clearly showed that the increase of thermal diffusivity can be ascribed to crack healing and sintering neck formation. Similar results on crack healing and sintering neck formation during the sintering of TBC have been found in previous investigations [25–27].

4. Conclusion

The isothermal oxidation test result indicates that the oxidation kinetics of nanostructured TBC obeys a parabolic law and the oxidation resistance of the nanostructured TBC is comparable to that of the conventional TBC. The nanostructured thermal barrier coatings exhibited excellent thermal cyclic resistance and low thermal diffusivity. The failure of the nanostructured TBC occurs within the top coat and close to the YSZ/thermal growth oxide interface. The thermal diffusivity of the coating is 90% of that of conventional thermal barrier coatings, and is increased after heat treatment at 1050 °C for 34 h. The increase in thermal diffusivity of the coating increases is ascribed to grain growth, the crack healing and sintering neck formation.

Acknowledgements

This work is supported by the National Natural Science Foundation of China under the contact 50176005, the Aviation Science Foundation of 2008ZE51073, Program for New Century Excellent Talents in University (NCET) and the Innovation Foundation of BUAA for PhD Graduates.

References

[1] H.X. Chen, M. Zhou, C.X. Ding, Investigation of the thermomechanical properties of a plasma-sprayed nanostructured zirconia coating, J. Eur. Ceram. Soc. 23 (2003) 1449–1455.
[2] C.G. Zhou, N. Wang, S.K. Gong, H.B. Xu, Heat treatment of nanostructured thermal barrier coating, Ceram. Int. 33 (2007) 1075–1081.
[3] M. Gell, Application opportunities for nanostructured materials and coatings, Mater. Sci. Eng. A 204 (1995) 246–251.
[4] J. Karthikeyan, C.C. Berndt, J. Tikkanen, S. Reddy, H. Herman, Plasma spray synthesis of nanomaterial powders and deposits, Mater. Sci. Eng. A 238 (1997) 275–286.
[5] H. Chen, C.X. Ding, Nanostructured zirconia coating prepared by atmospheric plasma spraying, Surf. Coat. Technol. 150 (1) (2002) 31–36.
[6] R.S. Lima, A. Kucuk, C.C. Berndt, Evaluation of microhardness and elastic modulus of thermally sprayed nanostructured zirconia coatings, Surf. Coat. Technol. 135 (2001) 166–172.
[7] M. Gell, L.D. Xie, X.Q. Ma, E.H. Jordan, N.P. Padture, Highly durable thermal barrier coatings made by the solution precursor plasma spray process, Surf. Coat. Technol. 177–178 (2004) 97–102.
[8] L.D. Xie, X.Q. Ma, E.H. Jordan, N.P. Padture, D.T. Xiao, M. Gell, Deposition mechanisms of thermal barrier coatings in the solution precursor plasma spray process, Surf. Coat. Technol. 177–178 (2004) 103–107.
[9] L.D. Xie, D.Y. Chen, E.H. Jordan, A. Ozturk, F. Wu, X.Q. Ma, B.M. Cetegen, M. Gell, Formation of vertical cracks in solution-precursor plasma-sprayed thermal barrier coatings, Surf. Coat. Technol. 201 (2006) 1058–1064.
[10] R.A. Miller, Oxidation-based model for thermal barrier coating life, J. Am. Ceram. Soc. 67 (1984) 517–521.
[11] R.C. Pennefather, D.H. Boone, Mechanical degradation of coating systems in high-temperature cyclic oxidation, Surf. Coat. Technol. 76–77 (1995) 47–52.
[12] S. Sacre, U. Wienstorth, H.G. Feller, L.K. Thomas, Influence of the phase compositions on the transient-stage high-temperature oxidation behaviour of an NiCoCrAlY coating material, J. Mater. Sci. 28 (1993) 1843–1848.
[13] K.A. Khor, Y.W. Gu, Thermal properties of plasma-sprayed functionally graded thermal barrier coatings, Thin Solid Films 372 (2000) 104–113.
[14] R.E. Taylor, X. Wang, X. Xu, Thermophysical properties of thermal barrier coatings, Surf. Coat. Technol. 120–121 (1999) 89–95.
[15] C.G. Zhou, N. Wang, Z.B. Wang, S.K. Gong, H.B. Xu, Thermal cycling life and thermal diffusivity of a plasma-sprayed nanostructured thermal barrier coating, Scripta Mater. 51 (2004) 945–948.
[16] R.S. Lima, A. Kucuk, C.C. Berndt, Bimodal distribution of mechanical properties on plasma sprayed nanostructured partially stabilized zirconia, Mater. Sci. Eng. A 327 (2002) 224–232.
[17] J. Wu, H.B. Guo, L. Zhou, L. Wang, S.K. Gong, Microstructure and thermal properties of plasma sprayed nanostructure YSZ thermal barrier coatings, J. Therm. Spray. Technol. 19 (6) (2010) 1186–1194.
[18] G.C. Chang, W. Phucharoen, R.A. Miller, Finite element thermal stress solutions for thermal barrier coatings, Surf. Coat. Technol. 32 (1987) 307–325.
[19] K.J. Lawson, J.R. Nicholls, D.S. Rickerby, The effect of coating thickness on the thermal conductivity of CVD and PVD coatings, 4th International Conference on Advanced in Surface Engineering, Newcastle, UK, 1996 .
[20] L.T. Kabacoff, Thermal sprayed nano-structured thermal barrier coatings, NATO Workshop on Thermal Barrier Coatings, Aaalborg, Denmark AGARD-R-823, 1998, p. 12.
[21] G. Soyez, J.A. Eastman, L.J. Thompson, G.-R. Bai, P.M. Baldo, A.W. McCormick, Grain-size-dependent thermal conductivity of nanocrystalline yttria stabilized zirconia films grown by metal-organic chemical vapor deposition, Appl. Phys. Lett. 77 (8) (2000) 1155–1157.

[22] H. Zhou, F. Li, J. Wang, B.D. Sun, Microstructure analyses and thermophysical properties of nanostructured thermal barrier coatings, J. Coat. Technol. Res. 6 (2009) 383–390.
[23] N. Wang, Thermophysical Properties Failure Behavior of nanostructured Thermal Barrier Coatings, Master Degree Thesis, Beijing University of Aeronautics and Astronautics, 2006.
[24] F. Cernuschi, L. Lorenzoni, S. Ahmaniemi, P. Vuoristo, T. Mantyla, Modified thick thermal barrier coatings: thermophysical characterization, J. Eur. Ceram. Soc. 24 (2004) 2669–2679.
[25] B. Siebert, R. Vassen, D. Stover, Changes in porosity and Young's modulus due to sintering of plasma sprayed thermal barrier coatings, J. Mater. Process. Technol. 92–93 (1999) 217–223.
[26] H.E. Eaton, R.C. Novak, Sintering studies of plasma-sprayed zirconia, Surf. Coat. Technol. 32 (1987) 227–236.
[27] V. Lughi, V.K. Tolpygo, D.R. Clarke, Microstructural aspects of the sintering of thermal barrier coatings, Mater. Sci. Eng. A 368 (2004) 212–221.